Etching of Si through a thick condensed XeF2 layer

Please check the document version of this publication:

• A submitted manuscript is the version of the article upon submission and before peer-review. There can be important differences between the submitted version and the official published version of record. People interested in the research are advised to contact the author for the final version of the publication, or visit the DOI to the publisher's website.
• The final author version and the galley proof are versions of the publication after peer review.
• The final published version features the final layout of the paper including the volume, issue and page numbers.

Link to publication

Etching of Si through a thick condensed XeF$_2$ layer

P. G. M. Sebel, L. J. F. Hermans, and H. C. W. Beijerinck[a)]
Physics Department, Eindhoven University of Technology, 5600 MB Eindhoven, The Netherlands

Etching of silicon by XeF$_2$ is studied in a multiple-beam setup. Below 150 K XeF$_2$ condenses and forms a layer on the silicon, which blocks the etching. Upon ion bombardment, this layer is removed and etching will resume. As a function of the layer thickness, the various removal mechanisms of the layer are studied. For a thick condensed layer it is found that 1 keV Ar$^+$ ions sputter the condensed layer with a yield of 160 XeF$_2$ molecules per ion for 1 keV Ar$^+$ ions and 280 for 2 keV ions. For thinner layers (below 9 nm for 1 keV ions), this sputter rate by ions decreases significantly. Here, the removal is mainly due to consumption of XeF$_2$ by etching at the bottom of the layer. This consumption rate reaches a maximum for a layer thickness of about 5 nm. In the steady-state situation, the layer thickness is further decreased, resulting in a smaller consumption and etch rate. Here, sputtering is the most important removal mechanism for the deposited XeF$_2$ layer. From this, it is concluded that a pulsed ion beam should be used in cryogenic etching to obtain the highest etch rate. © *2000 American Vacuum Society.* [S0734-2101(00)07005-6]

I. INTRODUCTION

For etching of SiO$_2$, fluorocarbon gases are usually applied because of their high etch rate and high selectivity.[1] Etching then occurs through a CF$_x$ fluorocarbon film, deposited on top of the material. In the absence of ion bombardment, the film thickness grows and the surface is passivated. Upon ion bombardment, first the CF$_x$ layer is removed from the surface and subsequently etching begins. Depending on process conditions and material, CF$_x$ film thicknesses ranging from 1 nm (for SiO$_2$) to 7 nm (for Si) were measured on a sample in a steady-state etching situation.[2] This selective CF$_x$ deposition on various materials is believed to be the key mechanism for selective etching. The etch rate is inversely proportional to the thickness of this fluorocarbon film.[3] Because of the importance of this passivating film, many of its characteristics have been studied.[3] From these studies, models have been proposed to explain the transport of etchant flux (both neutrals and ions) and reaction products (e.g., SiF$_4$) through a passivating layer.[2]

The etching of Si under cryogenic conditions has already been studied for several gases.[4–6] For example, Mullins and Coburn[4] concluded that Si etching by F atoms is blocked by Si$_2$F$_6$ at 77 K. However, in none of these experiments were results presented of the etching process after a thick layer of condensed gases had been deposited on the surface.

To expand the knowledge about etching through passivating films, we studied the etching of Si through a condensed XeF$_2$ layer. As shown by Vugts *et al.*,[7,8] XeF$_2$ condenses on Si at $T = 150$ K. Similar to a CF$_x$ layer, the XeF$_2$ layer blocks the etching of Si. Upon ion bombardment first the passivating layer is removed after which etching is observed. In this article the removal rate by the ions and the consumption rate of the XeF$_2$ layer due to etching are studied as a function of the thickness of the condensed layer.

After a brief description of the setup a typical measurement of the formation and removal of the condensed XeF$_2$ layer and its influence on the etch behavior is presented in Sec. III. From this, the consumption and sputter rate as a function of the thickness of the condensed layer are determined when the layer is removed to reach a steady-state. This forms the main part of the article. In Sec. IV the observation that the time to reach a steady state increases with the initial deposited layer thickness is explained. In Sec. V the experimental results are discussed. Finally, in Sec. VI the results for a condensed XeF$_2$ layer are compared with the measurements for a CF$_x$ layer, together with some general concluding remarks on experimental results.

II. EXPERIMENT

A. Multiple-beam setup

The multiple-beam setup used in our work is the same as described by Vugts *et al.*[9] The silicon sample is placed at the intersection of the XeF$_2$ beam and the Ar$^+$ beam in an ultrahigh vacuum (UHV) chamber (5×10^{-8} mbar) (Fig. 1). On one side the Si(100) sample (*n* type, phosphorus, 30–70 Ω cm) is clamped on the sample holder by a nickel retainer plate. The samples are cleaned with HF to remove native oxide before being mounted. The XeF$_2$ beam and Ar$^+$ beam are incident under 52° and 45°, respectively, with respect to the surface normal. The sample is connected to an electrometer to measure the ion current. To raise the temperature of the sample, a Thermocoax heating wire is wound around the sample holder. For cooling the sample below room temperature, the sample holder is also connected to a liquid nitrogen vessel by braided copper wire. In this way the temperature can be controlled in the range from 100 to 800 K. The temperature is measured by an alumel/chromel thermocouple, which is placed 1 mm behind the sample. In this work the sample temperature is $T = 130$ K.

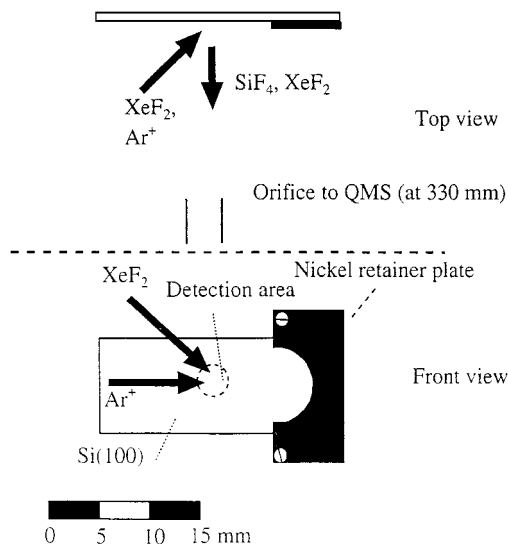The XeF$_2$ gas is supplied by a multicapillary effusive gas

---

FIG. 1. Experimental setup (front and top view). The Si sample is clamped by a nickel retainer plate. The different gas flows are incident from the left and the mass spectrometer is positioned perpendicular to the Si at 330 mm from the sample in a differentially pumped chamber.

source. During the experiments a XeF_2 flux of $\Phi_s(XeF_2)=0.55$ ML s^{-1} is used. For silicon 1 ML corresponds to a surface density of 6.86×10^{18} m^{-2}. The Ar$^+$ ions in the range of 0.5–2.5 keV are produced in a Kratos WG 537 Macrobeam ion gun and its shape is well described by a Gaussian profile with a full width at half maximum of 5 mm. From this it is calculated that an ion current of 1 μA corresponds to an average ion flux of 0.011 ML s^{-1} on the 3 mm diam area viewed by the mass spectrometer. In the experiment, ion currents of 0.65 and 1.35 μA were used, which correspond to an ion flux of $\Phi_s(Ar^+)=(7.2\pm0.7)10^{-3}$ ML/s and $\Phi_s(Ar^+)=(1.5\pm0.1)10^{-2}$ ML/s, respectively.

B. Structure of XeF₂

XeF_2 is a symmetric linear molecule and the Xe–F bond is 1.98 Å. The crystal structure of XeF_2 is tetragonal, with lattice parameters $a=4.315$ and $c=6.990$ Å.[10,11] The molecules are aligned along the c axis (Fig. 2). From these parameters and two molecules per cell, a density of 4.32 g/cm^3 is calculated.[10] It is also calculated that 1 ML XeF_2 corresponds to a thickness of 4.47 Å. It is noted that the unit ML in this article refers to the surface density of Si [1 ML(Si)$=6.86\times10^{18}$ m^{-2}]. The surface density for XeF_2 is 1 ML(XeF_2)$=3.31\times10^{18}$ m^{-2} and corresponds to a XeF_2 layer thickness of 2.158 Å.

However, it is unlikely that a perfect crystalline structure will form when XeF_2 condenses on a rough Si surface. Despite this, we will assume a perfect crystal structure to calculate the thickness of the condensed XeF_2 layer in the experiments.

C. Process coefficients

The etch reaction is monitored by a quadrupole mass spectrometer (QMS) in a separate UHV chamber
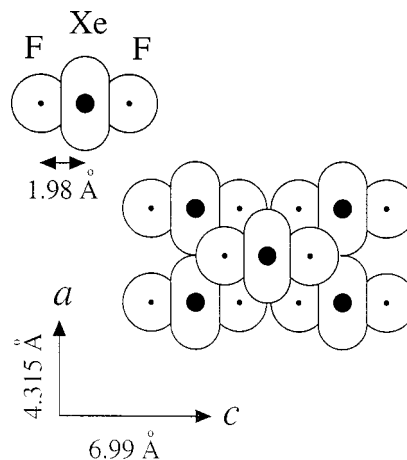

FIG. 2. Structure of XeF_2: single XeF_2 molecule and the structure of the XeF_2 crystal. The small and large dots indicate the F and Xe atoms, respectively. The circles and ellipses around the atoms indicate the interaction spheres of the F$^-$ and Xe^{2+} ions.

($<10^{-8}$ mbar) positioned along the surface normal of the sample (Fig. 1), at a position 330 mm downstream of the sample. The central detection area seen by the QMS is 3 mm in diameter. With the mass spectrometer, the nonreacted XeF_2 signal $I(XeF^+)$ and the SiF_4 signal $I(SiF_3^+)$ are measured. The XeF_2 signal $I(XeF^+)$ is calibrated by measuring the XeF_2 diffusively scattered from the nickel at room temperature. We consider the nickel surface as an inert, diffuse scatterer and thus this signal corresponds to the incident XeF_2 flux $\Phi_s(XeF_2)$. The nonreacted flux $\Phi(XeF_2)$ from the Si yields the reaction probability ϵ of XeF_2 at room temperature

$$\epsilon=\frac{\Phi_s(XeF_2)-\Phi(XeF_2)}{\Phi_s(XeF_2)}=0.17\pm0.02. \tag{1}$$

In a similar way, the SiF_4 production coefficient δ_4 is defined as

$$\delta_4=\frac{4\Phi(SiF_4)}{2\Phi_s(XeF_2)}. \tag{2}$$

In the case of spontaneous etching at room temperature SiF_4 is the only reaction product.[7] This enables us to calibrate the SiF_4 signal $I(SiF_3^+)$ to the production coefficient δ_4, by applying a fluorine mass balance

$$\delta_4=\epsilon. \tag{3}$$

To correct for the temperature-dependent detection probability, it is assumed that 85% of the signal consists of species with the sample temperature T.[9] Thus, in order to be able to use the calibration at room temperature T_{room}, all measured signals $I(T)$ at a sample temperature T are corrected to I_{corr}

$$I_{corr}=I(T)\left(0.15+0.85\sqrt{\frac{T_{room}}{T}}\right)^{-1}. \tag{4}$$

When the Si sample is cooled to 130 K, the XeF_2 condenses on the surface and blocks the etching. Now the fluorine mass balance of Eq. (3) no longer applies and the reac-
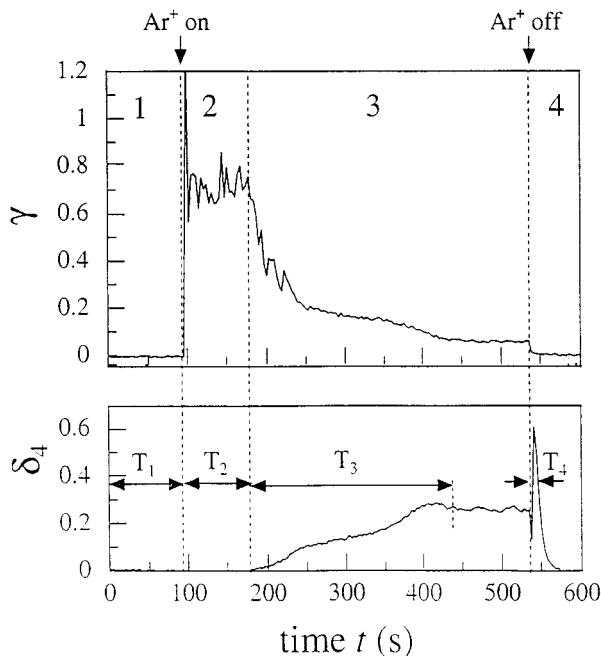
FIG. 3. Measured XeF$_2$ and SiF$_4$ signal coefficients γ and δ_4, respectively, during the removal of a XeF$_2$ layer of 200 ML and subsequent etching at a sample temperature of $T=130$ K. The XeF$_2$ beam is continuous while the Ar$^+$ beam is switched on/off as indicated. In stage 2 only a XeF$_2$ signal is observed. After $\Delta t = T_2$ a SiF$_4$ signal is measured, indicating that Si is etched. After $\Delta t = T_3$, a steady state is reached. In stage 4 the ion beam is switched off again. The XeF$_2$ signal immediately drops to zero, while in the SiF$_4$ signal first a peak is measured, before it drops to zero.

tion coefficient ϵ is no longer a true reaction coefficient. To describe the XeF$_2$ signal at this temperature, the XeF$_2$ reflection coefficient γ is introduced

$$\gamma = \frac{\Phi(\text{XeF}_2)}{\Phi_s(\text{XeF}_2)}. \tag{5}$$

The case $\gamma=0$ corresponds to a sticking probability equal to unity, while $\gamma=1$ corresponds to a situation when no net XeF$_2$ remains on the surface.

III. EXPERIMENTAL RESULTS AND INTERPRETATION

A. Typical result

In Fig. 3 the signal coefficients γ and δ_4 are shown when the ion bombardment is switched on after a XeF$_2$ layer of 200 ± 20 ML XeF$_2$ has been condensed on the surface. The ion current is 1.35 μA (i.e., 0.015 ML/s). The behavior of γ and δ_4 is divided into four distinct stages. In the first stage, the XeF$_2$ condenses on the surface during a time interval T_1. Both γ and δ_4 are zero, indicating a sticking probability of unity and no etching. In the second stage the ion bombardment is started on the condensed XeF$_2$ layer, but no SiF$_4$ signal is measured. The XeF$_2$ signal γ obviously results from species which are removed from the condensed layer. It was observed that this XeF$_2$ signal is very unstable during the sputtering of the condensed layer. This instability is charac-

teristic for the sputtering of a thick XeF$_2$ layer. After a time T_2, a SiF$_4$ signal is measured and the XeF$_2$ signal drops. This marks the end of stage 2.

In stage 3, SiF$_4$ is produced indicating Si etching under the influence of the ion bombardment. After a time T_3 the SiF$_4$ signal reaches steady state. Finally, in stage 4, the ion bombardment is switched off. The XeF$_2$ signal immediately drops to zero. The SiF$_4$, however, first increases above the steady-state signal under ion bombardment before it drops to zero, indicating condensation of XeF$_2$ on the surface. The peak in the SiF$_4$ production after ion switch off is explained by an increasing net influx of XeF$_2$ after the sputtering ceases, while the SiF$_4$ production is not yet limited by a condensed XeF$_2$ layer.

To model the removal and formation of the condensed layer, we use the following rate equation for the amount D_{XeF_2} (ML) of condensed XeF$_2$ on the surface.[3]

$$\frac{d}{dt}D_{\text{XeF}_2} = \Phi_s(\text{XeF}_2) - R_{\text{XeF}_2} - C_{\text{XeF}_2}. \tag{6}$$

Here, $\Phi_s(\text{XeF}_2)=0.55$ ML/s is the deposition rate of the XeF$_2$ layer (the sticking probability is unity because $\gamma=0$ in stage 1). Next, R_{XeF_2} is the sputter rate at the top of the condensed layer due to the ion bombardment and C_{XeF_2} is the consumption rate at the bottom of the condensed layer due to the etching of silicon. Thus C_{XeF_2} is proportional to the SiF$_4$ production. The sputter and consumption rates are functions of both the condensed layer thickness and the ion flux. Their sum gives the total removal rate of the condensed layer. Obviously, in a steady-state situation this removal rate becomes equal to the deposition rate $\Phi_s(\text{XeF}_2)$.

In the next sections we will investigate the behavior of the sputter and consumption rates as a function of the layer thickness D_{XeF_2} during ion bombardment. First the sputter rate is studied in the case of a semi-infinite layer thickness (stage 2). Next, the sputter and consumption rates are studied during etching (stage 3). Finally, the consumption rate is studied as a function of the layer thickness in the case of spontaneous etching (stage 4).

B. Removal of condensed XeF$_2$ layer (stage 2)

In stage 2, only a XeF$_2$ signal was observed (Fig. 3). Thus, the consumption rate is $C_{\text{XeF}_2}=0$. To study the sputter rate R_{XeF_2} of the condensed XeF$_2$ layer, the ion bombardment time T_2 needed to reach etching is measured as a function of the thickness of the deposited XeF$_2$ layer. We assume that the total layer condensed XeF$_2$ has been removed after $t=T_2$ (Fig. 3). In Sec. V we will come back to this assumption. In Fig. 4 the dose $D_{\text{Ar}^+}=\Phi_s(\text{Ar}^+)T_2$ to remove the layer with thickness D_{XeF_2} is shown for 1 keV Ar$^+$ ions and ion currents of 0.65 and 1.35 μA. It is seen that the ion dose increases linearly with the thickness of the layer for both ion fluxes, with an offset on the order of 20 ML. This means that for a layer thickness of less than 20 ML, a SiF$_4$ signal is measured immediately upon ion bombardment. For 2 keV an
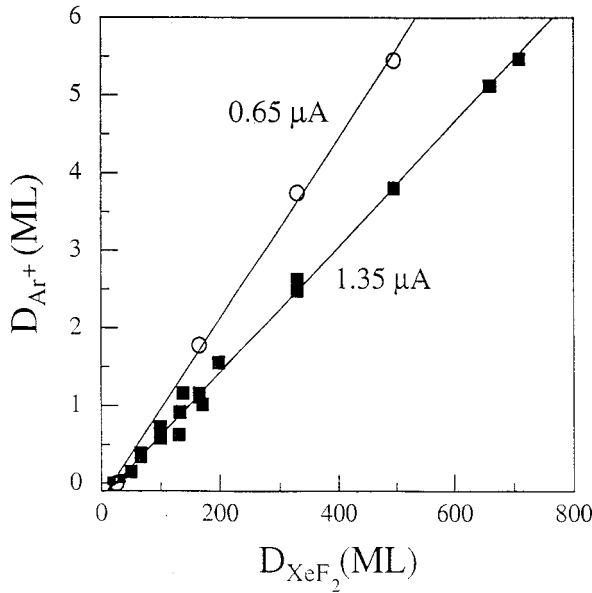
FIG. 4. Ion dose D_{Ar^+} to remove a layer D_{XeF_2} of condensed XeF₂. The results are shown for an ion current of 1.35 μA (closed squares) and 0.65 μA (open circles) at 1 keV. From the slope the net yield Y_{net} of removed XeF₂ molecules per incoming Ar⁺ is calculated.
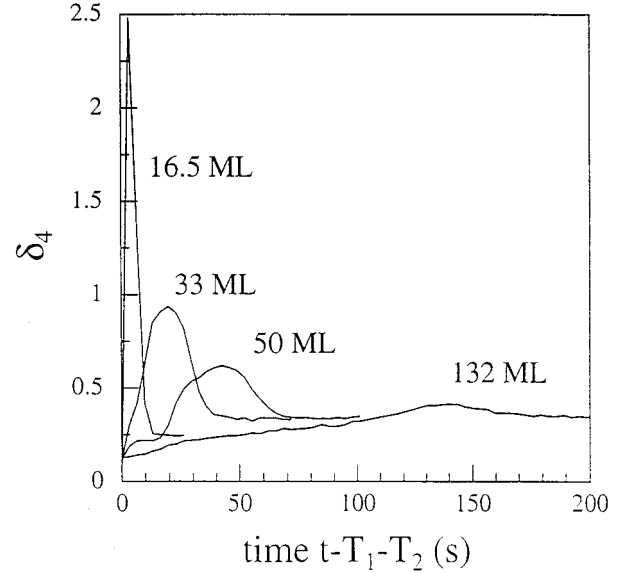

FIG. 5. Response of the SiF₄ production coefficient δ_4 to the onset of etching after time $T_1 + T_2$ for various thicknesses of the XeF₂ layer (stage 3 in Fig. 3). The signals are only plotted until a steady state is reached.

offset on the order of 100 ML was observed. This behavior indicates that for thick layers the sputter rate is independent of the condensed layer thickness.

In terms of our model [Eq. (6)], a layer with a thickness of D_{XeF_2} is removed in a time $t = T_2$. In view of the linear behavior, we write $R_{XeF_2} = R_\infty = Y \Phi_s(Ar^+)$, where R_∞ is the sputter rate for a semi-infinitely thick layer when no etching of Si is observed and Y defines the XeF₂ dose sputtered from the condensed layer per incident ion. Now, Eq. (6) may be written for stage 2 as

$$\frac{-D_{XeF_2}}{T_2} = \Phi_s(XeF_2) - Y\Phi_s(Ar^+) = -Y_{net}\Phi_s(Ar^+). \quad (7)$$

Here, Y_{net} is the net yield derived from the change in the thickness of the condensed layer while the XeF₂ beam was on, corresponding to the inverse slope of the lines in Fig. 4. Using Eq. (7) we can then determine the total yield Y. For 1 keV Ar⁺ ions, the yield is equal to $Y \approx 170$ for both ion fluxes (Table I). For increasing ion energy, the yield increases to $Y = 300$ at 2 keV.

From the yield Y for 1 keV ions, a threshold ion flux $\Phi_{thres}(Ar^+) = 3.2 \times 10^{-3}$ ML/s (0.3 μA) for an incident XeF₂ flux $\Phi_s(XeF_2) = 0.55$ ML/s is needed to counterbalance the incoming XeF₂ flux. In this case the condensed XeF₂ layer

does not grow, nor is it removed ($Y_{net} = 0$). This is in agreement with additional measurements of the upper limit of the ion flux for which no etching stage is reached (not shown here).

C. Etching of Si (stage 3)

After most of the XeF₂ layer has been removed from the surface, a SiF₄ signal is measured indicating that the Si surface is etched (Fig. 3). The subsequent behavior of the SiF₄ signal was found to depend on the initial dose D_{XeF_2} of the film deposited on the surface (Fig. 5). For an initial thickness of 17 ML, a peak of SiF₄ is measured and steady state is reached after 15 s. However, for an initial XeF₂ layer of 132 ML the signal increases slowly and steady state is reached only after a much longer time $T_3 = 150$ s. It is also seen that the peak broadens for increasing initial thicknesses.

In Sec. IV, it will be shown that the increase of T_3 with increasing ion flux is explained by a nonuniform removal of the condensed layer and is described by Poisson statistics in the number of incident ions per area.

In order to minimize the influence of Poison statistics when determining the sputter and consumption rates as a function of the thickness [Eq. (6)], we use the data for a thin initial XeF₂ layer of 17 ML. The behavior of δ_4 and γ is shown in Fig. 6. From the behavior of γ it is seen that almost no XeF₂ signal is detected. This indicates that the XeF₂ sputter yield decreases very sharply with decreasing layer thickness around a dose of 17 ML. This lower sputter rate for thin condensed layers is due to competition of SiF₄ formation with the process of sputtering, since a peak in the SiF₄ formation is observed with a maximum of $\delta_4 = 2.5$. This corresponds to a consumption rate of $C_{XeF_2} \approx 1.8$ ML/s, where it is assumed that besides SiF₄ SiF₂ is also produced. Following

TABLE I. Values of Y_{net}, Y, and Y_{cor} for two ion fluxes and ion energies.

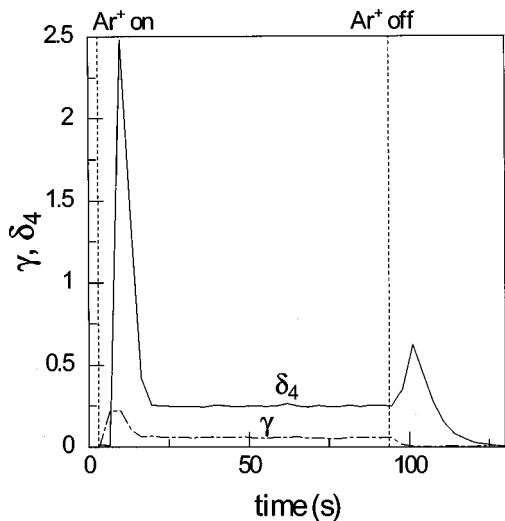| Ion energy (keV)	Ion current (μA)	Y_{net}	Y	Y_{cor}
1	0.6	90±9	167±17	159±17
1	1.35	133±13	170±17	157±17
2	1.25	263±26	300±30	280±30

FIG. 6. Response of the SiF$_4$ and XeF$_2$ signals when the ion bombardment (1.3 μA) is switched on after a layer of 17 ML was deposited on the surface.

the measurements of Vugts *et al.* we assume that 25% of the consumption results in SiF$_2$ formation and 75% in SiF$_4$ formation.[8]

The sputter and consumption rates as a function of the thickness D_{XeF_2} can be derived (Fig. 7) for an ion flux of $\Phi_s(Ar^+) = 0.015$ ML/s (1.35 μA) using the following data obtained above:

(1) For a very thick layer the sputter rate is $R_{XeF_2} = Y\Phi_s(XeF_2) = 2.4$ ML/s and $C_{XeF_2} = 0$.
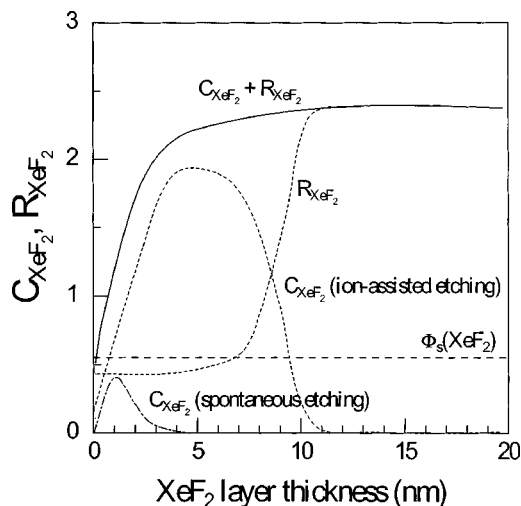

FIG. 7. Sputter rate R_{XeF_2} and consumption rate C_{XeF_2} of the XeF$_2$ layer for spontaneous and ion-assisted etching (for an ion flux of 1.35 μA). During ion-assisted etching, the XeF$_2$ layer is consumed at the bottom to produce etching for a XeF$_2$ layer of less than 9 nm. The consumption rate first increases with XeF$_2$ layer thickness after which it decreases sharply around a thickness of 9 nm. For layers thicker than 9 nm the layer is removed by sputtering from the top by the ion bombardment and no consumption at the bottom takes place. Steady state is reached when the removal rate $C_{XeF_2} + R_{XeF_2}$ is equal to the incoming XeF$_2$ flux $\Phi_s(XeF_2)$. During spontaneous etching, the consumption rate is lower than the incoming XeF$_2$ flux and shows a maximum around a layer thickness of 1 nm.

(2) For a layer thickness of about 9 nm (corresponding to a dose of 17 ML), the removal rate decreases and the consumption rate increases with decreasing layer thickness.
(3) The maximum consumption rate is $C_{XeF_2} = 1.8$ ML/s.
(4) In steady state the total consumption rate is $C_{XeF_2} = 0.18$ ML/s and the total removal rate $R_{XeF_2} + C_{XeF_2} = \Phi_s(XeF_2)$ which results in a sputter rate of 0.37 ML/s.

Furthermore, it is assumed that the remaining XeF$_2$ thickness $D_{XeF_2} = 0$, because no conclusions can be drawn from our measurements about the thickness of the XeF$_2$ layer in a steady-state situation. The resulting plot is shown in Fig. 7. It is noted that this is a construction of the removal and consumption rates. Thus, the plot only gives a rough description of the actual thickness dependence and no conclusions can be drawn from, e.g., the saturation point of the total removal rate around 3 nm.

D. Growth of condensed XeF$_2$ layer (stage 4)

As shown in Fig. 3, a peak in SiF$_4$ production is observed when the ions are switched off. The maximum height of the peak corresponds to $\delta_4 = 0.6$. The decay time of this peak varies from 6 to 30 s (at a continuous XeF$_2$ flux of 0.55 ML/s), depending on the sample history. These variations are attributed to surface roughness. For a rougher surface a thicker XeF$_2$ layer is needed to cover the whole surface. From the decay time of 6 s we conclude that a layer of about 7 ML XeF$_2$ is sufficient to stop the etching of silicon. This corresponds to a thickness of 3 nm. Since roughnesses on the order of 100 nm have been reported,[12] it is obvious that roughness will influence the experimental results.

From this observation, it is possible to construct a plot of the consumption rate C_{XeF_2} as a function of the layer thickness in the case of spontaneous etching (i.e., the sputter rate $R_{XeF_2} = 0$). Since a thick XeF$_2$ layer is formed on the surface, the consumption rate $C_{XeF_2} < \Phi_s(XeF_2)$. Similar to the consumption curve in the case of ion-assisted etching, now a maximum will also be observed. The maximum will occur for a layer of about 1 nm. After 3 nm (depending on the surface roughness) the consumption and thus the etching will cease. This consumption rate as a function of the layer thickness during spontaneous etching is included in Fig. 7.

IV. ION FLUX DEPENDENCE

In this section the behavior of Fig. 5 will be explained qualitatively in terms of Poisson statistics. The explanation does not revert back to Eq. (6) and thus contains no extra information on the sputter and consumption rate as a function of the layer thickness. At the end of this section this explanation will be shown to be corroborated by experiments.

A. Poisson statistics

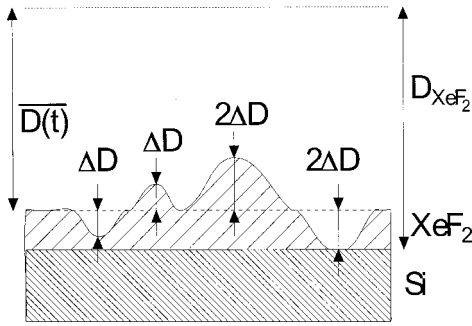It was observed that when a thicker film of XeF$_2$ is deposited, the δ_4 peak is broadened and T_3 increases (Fig. 5).

FIG. 8. Schematic of the sputtering of the condensed XeF$_2$ layer on the onset of etching. The dotted line at the top is the height of the XeF$_2$ layer when the ion bombardment is started (corresponding to a deposited dose D_{XeF_2}). Due to statistics in the number of ions incident on the surface area, differences in height Δd form on the surface. The highest peaks are on the order of $2\Delta d$ and the height differences over the surface are on the order of $4\Delta d$.
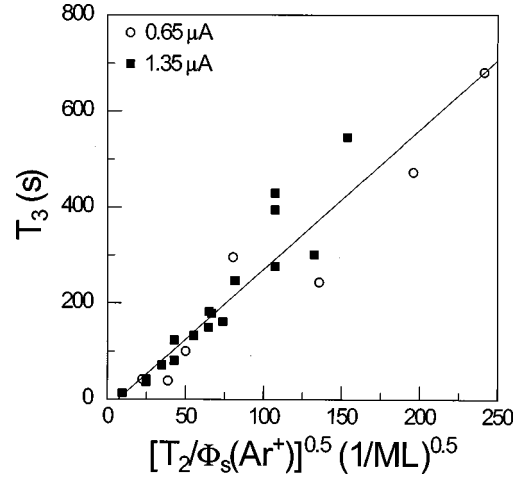

FIG. 9. Time T_3 to reach a steady-state SiF$_4$ signal under ion bombardment as a function of the square root of the sputter time T_2 per unit ion flux $\Phi_s(Ar^+)$. Measurements with an ion current of 1.35 μA (squares) and 0.65 μA (circles) are shown. A linear dependence between both variables is measured (line).

A similar effect as a function of the film thickness was measured in the sputtering of condensed H$_2$ by 5 keV H$^+$ [13] and the sputtering of condensed CO by 1 keV Ar$^+$.[14] Indeed, Fig. 5 is almost identical to the results of the H$_2$ signal as a function of the bombardment time for various initial thicknesses of the H$_2$ condensate.[13] Chrisey *et al.* explained the broadening of the peak of sputtered CO near the surface to be a nonuniform removal of the condensed layer.[14] Below it is shown that the nonuniform removal in our experiment can be described by assuming Poisson statistics in the number of ions arriving at the surface.

Because of the low ion flux (on the order of 1–2 ions/s per area of 10 by 10 Si atoms) and the high yield, statistics in the number of ions will result in a spread of the XeF$_2$ layer thicknesses over the surface (Fig. 8). Etching starts at a spot on the surface where all XeF$_2$ has been locally removed. A steady-state situation is then reached when the XeF$_2$ has been removed from the entire surface. Thus, the driving mechanism for the variations in the XeF$_2$ layer height can be the Poisson statistics in the ion bombardment. Using a simple model we will try to quantify this picture.

The average dose XeF$_2$ $\overline{D(t)}$ removed by the ion bombardment, is given from Eq. (7) by

$$\overline{D(t)} = Y_{net}\Phi_s(Ar^+)t. \qquad (8)$$

To calculate the number of ions arriving at the surface, we assume that each ion affects an area A (ML^{-1}) of the surface. The area A can be expressed in terms of the number of surface XeF$_2$ molecules capping the volume that is removed by one ion. As a total of Y molecules per ion is removed from the surface, the capping area A is on the order of $A \approx Y^{2/3} = 30.7$/ML of incident ions, when we assume that a cube-shaped volume of atoms is removed by an incident ion. The average number $\bar{N}$ of incident ions on such an area A is given by

$$\bar{N} = \Phi_s(Ar^+)At. \qquad (9)$$

The spread ΔN in this number is given by Poisson statistics

$$\Delta N = \bar{N}^{1/2} = [\Phi_s(Ar^+)At]^{1/2}. \qquad (10)$$

The corresponding spread ΔD in removed layer thicknesses after sputtering for a time $t = T_2$ is now

$$\Delta D/\overline{D(t)} = \Delta N/\bar{N} = [\Phi_s(Ar^+)AT_2]^{-1/2}. \qquad (11)$$

To determine whether these variations in thickness are of importance, we calculate these variations for some characteristic numbers. We take $A \approx 30$ ML^{-1} and $\Phi_s(Ar^+)T_2 \approx 3$ ML (Fig. 4). For these numbers the spread in thickness is on the order of 10% for a XeF$_2$ layer of 400 ML.

These variations in the sputtered thickness are shown schematically in Fig. 8 at the onset of etching. Steady state is reached when all the highest peaks are removed from the surface, measured from the lowest points. This thickness is assumed to be on the order of $4\Delta D$, accounting for 95% of all XeF$_2$ species still remaining on the surface. The time T_3 to remove this thickness is now calculated by using Eqs. (8) and (11)

$$T_3 = \frac{4\Delta D}{Y_{net}\Phi_s(Ar^+)} = \frac{4}{A^{1/2}}[T_2/\Phi_s(Ar^+)]^{1/2}. \qquad (12)$$

In Fig. 9, the measurements of T_3 are plotted as a function of $[T_2/\Phi_s(Ar^+)]^{1/2}$ for two different ion fluxes. We see that the linear dependence expected from Eq. (12) applies quite well to the measurements of both ion fluxes and that the results of both ion fluxes now coincide. However, from the fit we find that the proportionality factor $4/A^{1/2} = 2.9$. The corresponding value of $A = 1.9$ would suggest that an ion removes a surface area of 1.9 atoms to a depth of 89 ML. We conclude that this is an unrealistically small value of A when compared to the expected value on the order of $A \approx 30$.

A possible explanation for this discrepancy is the following. In the calculation it is assumed that the XeF$_2$ is sputtered from the surface with the same characteristics over the whole range. It was, however, already shown that the last 20 ML of condensed XeF$_2$ are not sputtered from the surface, but Si is etched through this layer while consuming it. Different char-
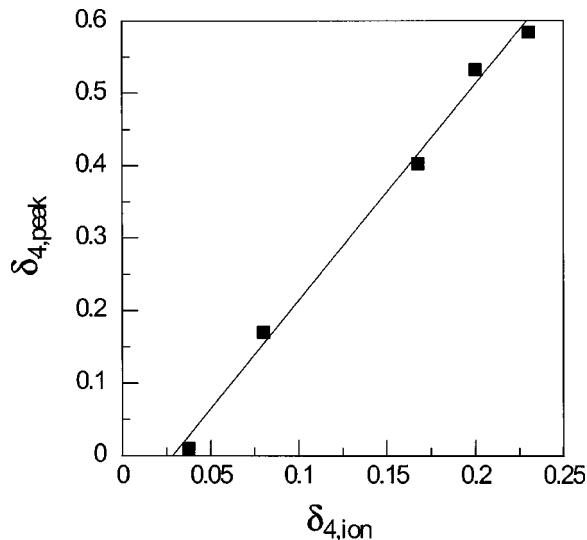
FIG. 10. Peak value of the SiF$_4$ signal δ_{peak} when the ions are switched off as a function of the SiF$_4$ signal $\delta_{4,ion}$ at the moment of switch off. A SiF$_4$ production coefficient $\delta_4 = 0.25$ is the steady state during ion-assisted etching.

acteristics for the removal of this last layer might explain the observed discrepancy in the value of A. In addition, variations in the simultaneous deposition of XeF$_2$ are not included. It might well be possible that the XeF$_2$ deposits preferably on the surface peaks, thus increasing the time to remove the remaining differences in height.

B. Verification

We conclude that the XeF$_2$ is removed nonuniformly from the surface and islands (crystals) of condensed XeF$_2$ remain on the surface. Etching only occurs on sufficiently thin surface spots, where the etching is not blocked by a condensed XeF$_2$ layer. As a consequence, spontaneous SiF$_4$ production when the ion beam is switched off (stage 4 in Fig. 3) is only possible on these open areas. Thus, the SiF$_4$ peak height after ion switch off should be linearly proportional to the SiF$_4$ production just before ion switch off.

The above reasoning is confirmed by an experiment in which the ion flux is interrupted when the SiF$_4$ signal has *not yet reached* steady state, i.e., during stage 3 in Fig. 3. The result of the subsequent SiF$_4$ peak height is shown in Fig. 10. These measurements were done after an initial layer of 330 ML XeF$_2$ was deposited. The ion flux is 0.015 ML/s. It is seen that the peak height $\delta_{4,peak}$ increases linearly with the SiF$_4$ signal $\delta_{4,ion}$ at ion switch off. When the ions are switched off immediately after the first SiF$_4$ signal is observed, the SiF$_4$ production decreases to zero within 0.1 s and no peak is measured (offset in Fig. 10). This immediate drop in the SiF$_4$ signal just after etching has started is always observed, independent of the initial XeF$_2$ layer thickness. For example, this decrease is also found when the ions are switched off at the peak value of the SiF$_4$ production for an initial XeF$_2$ layer of 17 ML (Fig. 5).

This behavior confirms the observation that etching first takes place through a condensed layer: the consumption rate during ion-assisted etching extends to thicker layers (9 nm) than during spontaneous etching (3 nm).

V. DISCUSSION

A. Sputter rate of XeF$_2$

In the calculation of the yield Y, it was assumed that all of the condensed XeF$_2$ layer has been removed before the first SiF$_4$ signal is detected. However, in Sec. IV it was shown that the first SiF$_4$ signal is already detected when a layer $\bar{D} = D_{XeF_2} - 2\Delta D$ (Fig. 8) has been removed from the surface. Thus, the total dose removed from the surface is lower than the total condensed dose D_{XeF_2}. As a consequence, the calculated yields are too high (Table I). The corrected yield Y_{cor} is calculated using Eq. (11) with $A = 30$ and included in Table I.

The yields of 160 and 280 for 1 and 2 keV ions, respectively, may seem very large compared to the normal yields on the order of 0.1–10 for metals and semiconductors. The explanation for this difference is the low binding energy (0.03–0.5 eV) of the condensed molecules, where only van der Waals forces apply. This binding energy is at least one order of magnitude smaller than those of metals.[15] Sputter yields for other condensed gases are on the same order of magnitude as the measured yields. For example, the yield of 1 keV Ar$^+$ ions on condensed Ar, Kr, and Xe layers is 412, 191, and 92, respectively.[16] For condensed molecules, a yield on the order of 500 was reported for 6 keV Ar$^+$ ions on condensed CH$_4$,[17] and a yield of 26 for 1 keV Ar$^+$ ions on condensed SiCl$_4$.[4]

In our measurements, the measured XeF$_2$ signal corresponds to an apparent XeF$_2$ flux leaving the surface of $\gamma\Phi_s(XeF_2) = 0.39$ ML/s (Fig. 3), while a true flux $\Phi(XeF_2) = Y\Phi_s(Ar^+) = 2.52$ ML/s is removed from the surface. This indicates that the XeF$_2$ signal is a factor of 6.5 too low. This discrepancy is also observed for steady state, where $\gamma = 0.1$ is observed (indicating that 10% of the XeF$_2$ is sputtered), whereas the production only accounts for the consumption of 35% of the XeF$_2$. Thus, here also a factor of 6.5 is missing, when it is assumed that there is a systematic error in γ. Of course, this could be due to ion-induced sputtering of XeF$_2$. However, since the XeF$_2$ sputter rate is determined from the XeF$^+$ mass spectrometer signal, ion-induced dissociation is included in γ. Looking at the ratio of the XeF$^+$ and XeF$_2^+$ mass spectrometer signals as a function of temperature by Vugts *et al.*,[8] we conclude that ion-induced sputtering of XeF$_2$ cannot explain the factor of 6.5.

We explain the observed discrepancy by a combination of two factors. The first one is the smaller detection probability of the faster-than-thermal XeF$_2$ molecules leaving the 130 K surface and the second is the transfer of momentum from the ions incident at 45° to the sputtered XeF$_2$ species, which leads to an angular distribution outside the acceptance of the mass spectrometer, which is mounted perpendicular to the sample.

B. Comparison with a CF$_x$ layer

It is clear that a XeF$_2$ layer is different from a CF$_x$ layer in the way it blocks the etching. The XeF$_2$ layer really blocks the spontaneous etching. During ion bombardment, etching can occur through a layer on the order of 9–45 nm thick, depending on the ion energy, but in a steady state no thick protective layer covers the surface. The CF$_x$ layer, by contrast, acts as a reaction layer in a steady state to supply reactants to form reaction products. This is clearly shown in the case of Si, where diffusion of Si through the CF$_x$ layer is the etching mechanisms.[2]

The fundamental difference is that etching through a CF$_x$ layer is limited by reaction product *formation* while the etching through a XeF$_2$ layer is limited by the *release* of the reaction products.

VI. CONCLUDING REMARKS

When XeF$_2$ is deposited on Si, XeF$_2$ layers on the order of 3.3 ML ($\approx$1.5 nm) block the spontaneous etching of Si. This layer can be removed by ion bombardment. For thick layers, the layer is sputtered by the ions with a yield of 160 ± 17. For thickness thinner than 9 nm (when sputtering with 1 keV ions), the layer is mainly removed due to consumption of XeF$_2$ which results in etching. For even thinner layers, sputtering of XeF$_2$ becomes the most important removal mechanism again. For 2 keV the consumption takes place for layers with a thickness of less than 45 nm and the sputter yield for thick layers increases to 280 ± 30.

During spontaneous etching, the consumption only takes place for layers of less than 3 nm, which is much smaller than for ion-assisted etching. This is confirmed by the observation that no δ_4 peak is observed when the ion bombardment is ceased after the first SiF$_4$ signal is measured.

From the observation that the consumption is the most important removal mechanism for layers in the range of 2–9 nm, it is concluded that one should use a pulsed ion beam to obtain the highest etch rate. During the ion beam off cycle a layer on the order of 9 nm should be deposited which should subsequently be removed during the ion beam on cycle. Further it was concluded that no comparison could be made between etching through a CF$_x$ layer and a XeF$_2$ layer.

The observation that the time to reach a steady state situation increases for increasing initial layer thicknesses is explained by a nonuniform removal of the condensed layer. A simple model assuming Poisson statistics gives a good qualitative description of the observations, but fails to describe the correct time scale to reach a steady state.

[1] R. A. H. Heinecke, Solid-State Electron. **18**, 1146 (1975).
[2] T. E. F. M. Standaert, M. Schaepkens, N. R. Rueger, P. G. M. Sebel, G. S. Oehrlein, and J. M. Cook, J. Vac. Sci. Technol. A **16**, 239 (1998).
[3] M. Schaepkens, T. E. F. M. Standaert, N. R. Rueger, P. G. M. Sebel, G. S. Oehrlein, and J. M. Cook, J. Vac. Sci. Technol. A **17**, 26 (1999), and references cited herein.
[4] C. B. Mullins and J. W. Coburn, J. Appl. Phys. **76**, 7562 (1994).
[5] D. J. Oostra, A. Haring, A. E. de Vries, F. H. M. Sanders, and G. N. A. van Veen, Nucl. Instrum. Methods Phys. Res. B **13**, 556 (1986).
[6] R. B. Jackman, R. J. Price, and J. S. Foord, Appl. Surf. Sci. **36**, 296 (1989).
[7] M. J. M. Vugts, G. L. J. Verschueren, M. F. A. Eurlings, L. J. F. Hermans, and H. C. W. Beijerinck, J. Vac. Sci. Technol. A **14**, 2766 (1996).
[8] M. J. M. Vugts, L. J. F. Hermans, and H. C. W. Beijerinck, J. Vac. Sci. Technol. A **14**, 2820 (1996).
[9] M. J. M. Vugts, G. J. P. Joosten, A. van Oosterum, H. A. J. Senhorst, and H. C. W. Beijerinck, J. Vac. Sci. Technol. A **12**, 2999 (1994).
[10] S. Siegel and E. Gebert, J. Am. Chem. Soc. **85**, 241 (1963).
[11] S. Andersson, Acta Crystallogr., Sect. B: Struct. Crystallogr. Cryst. Chem. **35**, 1321 (1979).
[12] M. J. M. Vugts, M. F. A. Eurlings, L. J. F. Hermans, and H. C. W. Beijerinck, J. Vac. Sci. Technol. A **14**, 2780 (1996).
[13] S. K. Erentz and G. M. McCracken, J. Appl. Phys. **44**, 3139 (1973).
[14] D. B. Chrisey, W. L. Brown, and J. W. Boring, Surf. Sci. **225**, 130 (1990).
[15] G. Betz and K. Wien, Int. J. Mass Spectrom. Ion Processes **140**, 1 (1994).
[16] V. Balaji, D. E. David, T. F. Magnera, J. Michl, and H. M. Urbassek, Nucl. Instrum. Methods Phys. Res. B **46**, 435 (1990).
[17] R. Pedrys, D. J. Oostra, R. A. Haring, L. Calcagno, A. Haring, and A. E. de Vries, Nucl. Instrum. Methods Phys. Res. B **17**, 15 (1986).